Mater. Res. Soc. Symp. Proc. Vol. 1144 © 2009 Materials Research Society 1144-LL01-04

Growth of Ultra Thin ZnSe Nanowires

Tai-Lun Wong, Yuan Cai, Siu-Keung, Chan, Iam-Keong Sou and Ning Wang

Department of Physics and the William Mong Institue of Nano Science and Technology, The Hong Kong University of Science and Technology, Hong Kong, China

ABSTRACT

We report here the growth of ultra thin ZnSe nanowires at low temperatures by Au-catalyzed molecule beam epitaxy and structural characterization of the nanowires. ZnSe nanowires may contain a high density of stacking faults and twins from low temperature growth and show a phase change from cubic to hexagonal structures. Ultra thin ZnSe nanowires can grow at a temperature below the eutectic point, and the relationship between the growth rates and nanowire diameters is $V= 1/d^n+ C_0$ (C_0 is a constant and n is a fitting parameter). The growth rate of the ultra thin nanowires at low temperatures can be elucidated based on the model involving interface incorporation and diffusion, in which the catalyst is solidified, and the nanowire growth is controlled through the diffusion of atoms into the interface between the catalyst and nanowire. The growth rate of ZnSe ultra thin nanowires has been simulated.

INTRODUCTION

In the classical vapor-liquid-solid (VLS) model [1,2], it is believed that the metal catalyst is in molten state which absorbs the source materials to form a supersaturated liquid droplet. The precipitation of the source atoms occurs at the droplet-whisker interface, and the precipitation rate is mainly determined by the supersaturation of the droplet. Givargizov *et al.* [1,2] determined the whisker growth rate as a function of the driving force of supersaturation ($\Delta\mu/kT$) and first empirically described the growth rate by

$$V = \frac{dL}{dt} = b\left(\frac{\Delta\mu_o}{k_B T} - \frac{4\Omega\sigma}{dk_B T}\right)^n \quad (1),$$

where d is the nanowire diameter, T is the growth temperature, k_B is Boltzmann's constant $\Delta\mu_0$ is the effective difference between the chemical potentials of source element in the nutrient phase and in solid phase, Ω is the atomic volume source element, σ is the specific of the nanowire surface, b and n (~2) were empirical fitting parameters, . According to Equation (1), the larger the whisker diameter, the faster is its growth rate. This growth phenomenon is attributed to the well-known Gibbs-Thomson effect, i.e., the decrease of supersaturation as a function of the whisker diameter. [1, 2]

Due to the change of the driving force, Si whiskers with small diameters (< 100 nm) grow very slowly. Obviously, there is a critical diameter at which $\Delta\mu = 0$ and the whisker growth stops completely. Those whiskers with diameters less than the critical diameter (about 50nm) should stop growing. However, in recent years, both experimentalists and theorists [4-6] have showed that semiconductor nanowires with diameter smaller than 50 nm can grow and show interesting growth behaviors. For example, in the growth of thin

Si and ZnSe nanowires catalyzed by Au particles, thinner nanowires grow faster than thicker ones,[5,6] and most ultra thin nanowires grow at relatively low temperatures. Recently, using *in-situ* transmission electron microscopy (TEM), Kodambaka *et al.* [6] demonstrated that solid catalysts led to Ge nanowire growth even at a temperature below the eutectic point. In this paper, we present the structural changes of these nanowires grown at low temperatures by molecular-beam epitaxy (MBE) and their interesting growth behavior, which is totally different from that predicted by the classical VLS mechanism [1,2] or other growth models controlled by surface incorporation and diffusion mechanisms.[7]

EXPERIMENTAL DETAILS

ZnSe nanowires were grown by a VG V80H MBE system which was dedicated to ZnSe-based II-VI compound growth in a single chamber. A thin Au layer was deposited on a GaAs substrate at 150 °C and then annealed at 530 °C for 10 minutes in order to generate uniform Au nano-catalysts on the substrate surface. ZnSe nanowires were grown at different temperatures using a ZnSe compound source. Details of the experiment setup can be found in a previous paper.[8] The nanowire samples were prepared by cleaving the substrates into small pieces (without any chemical pretreatment) and directly characterized by TEMs (JEOL2010F and Philips CM120).

DISCUSSION

For the VLS growth, the temperature is critical to the nanowire quality and growth direction. [9] As shown in figure 1a, ZnSe nanowires formed at a temperature below 390 °C have non-uniform diameters at the initial growth stage. The nanowire roots are thicker than the tips, and the surfaces near the roots are rough. This is obviously because the deposition of ZnSe on the substrate surface is significant when the temperature is too low and these deposited atoms diffuse from the substrate surface to the nanowire growth fronts. ZnSe nanowires grown at a high temperature do not have this morphology. [8] Once the nanowires reach a certain length, there is no obvious change in the diameters. For the tapered nanowires shown in figure 1a, the diameters may change gradually from 30 nm at the roots to about 5 nm at the tops. The quality of the thick nanowires is poor in comparison with the nanowires grown at a higher temperature (> 530 °C). A high density of stacking faults and twins always occurs in these nanowires. Figure 1b illustrates the stacking faults and twinning structures observed in an individual nanowire. One of the reasons for the formation of these planar defects was due to the phase transformation from the face center cubic (FCC) structure to the hexagonal close-packed (HCP) structure. The chemical composition of the source materials, e.g. the evaporation ratio of Zn:Se and surface energies may also result in the formation of these defects.[10,11] We have observed that ZnSe nanowires formed at a temperature higher than 530 °C were always a cubic structure and contained few defects. Decrease of the growth temperature could result in a high density of stacking faults, nano twins and some portion of HCP structure. However, ultra thin ZnSe nanowires with diameters of about 3-6 nm are always perfect HCP structure at 390 °C (see figure 1c).

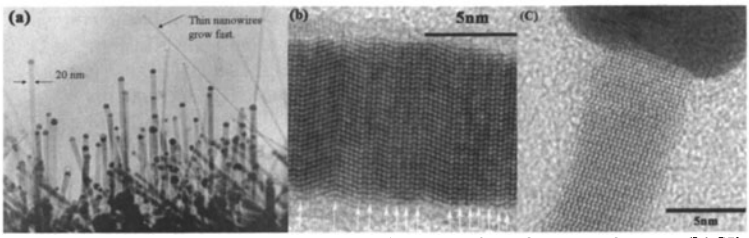

Figure 1(a). ZnSe nanowires with small diameters show fast growth rates. **(b)**.High-density stacking faults and twins (marked by the arrows) frequently occur in ZnSe nanowires grown at a low temperature. **(c).** Ultra thin ZnSe nanowires always form HCP structure.

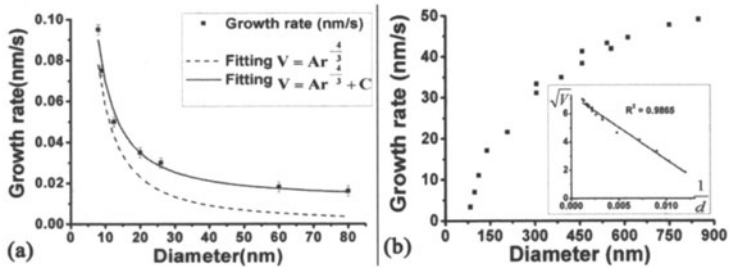

Figure 2(a). The solid dots indicate the growth rates measured from different diameters of ZnSe nanowires. The dashed line is the fitting curve by dL/dt=Ar-4/3 and the solid line by dL/dt=Ar-4/3+C. **(b).** Experimental data of the whisker growth rates reported by Givargizov (1975). [1]

From our measurement, the growth rate of thin ZnSe nanowires (diameters < 60 nm) displays a strong diameter-dependent phenomenon. Smaller nanowires have higher growth rates compared to thicker ones (see figure 2a). This is totally different from the growth of the nanowires or whiskers with diameters greater than 100 nm (see figure 2b, data from Ref. 2). Figure 2a illustrates the changes of growth rates versus the diameters of thin ZnSe nanowires. The relationship between the growth rates and the diameters can be described by $V= 1/d^n + C_0$ (C_0 is a constant and n is about 1-2).This relation does not agree with the classical VLS model,[1,2] in which the metal catalysts are liquid (above the eutectic point), and the nanowire growth is determined mainly by (i) the incorporation of the source atoms on the droplet, (ii) diffusion through the droplet and (iii) precipitation at the liquid-solid interface (see figure 3a). According to our TEM observation, for ultra thin nanowires, however, the growth may largely deviate from these three steps and also deviate from the growth model controlled by surface incorporation and diffusion mechanisms, i.e. the source materials captured by the droplet diffuse along the droplet surface to the growth front (see figure 3b). In this case, the growth rate can be described by V = 1/r [7]. This means that the growth rate is only determined by the circumference of the liquid-solid interface. Similar growth phenomena of diameter-dependence of

growth rates have been reported in III-V (e.g., GaAs, GaP, InAs and InP) nanowire growth by different methods, and the growth models based on surface diffusion mechanisms have been proposed. [12,13] For example, Froberg, et al. [12] has proposed a combined model which counts for both the Gibbs-Thomson effect and material diffusion from the substrate surface to explain the diameter-dependent growth rate of InAs nanowires. In their model, for those nanowires with diameters larger than 25nm, it is found that the growth rate is controlled by surface diffusion (the growth rate decreases with increasing the diameter). Due to the Gibbs-Thomson effect, when the nanowire diameters are smaller than 25nm, the growth rate decreases as the diameters shrink. This is because the driving force for the incorporation of atoms to the catalyst is reduced with decreasing the catalyst diameter. In this case, the catalyst is considered as a droplet if the temperature is sufficiently high.

For ultra thin nanowires, however, the growth temperatures are often lower than the eutectic point of the bulk material, and the catalyst may not be a droplet during growth. Due to the Gibbs-Thomson effect, the decrease of the catalyst droplet diameter lowers the solubility of the source atoms and thus shifts the melting temperature of the catalyst. For Au-semiconductor alloys (e.g., Au-Si, Au-Ge and Au-ZnSe), a deviation from the eutectic point generally causes the increase of the melting points. Since the growth of ultra thin nanowires can still maintain under the temperature below the eutectic point (the metal catalyst is solid) as observed by in-situ TEM,[6] the real incorporation and diffusion processes of the source atoms at nanowire tips are complicated.

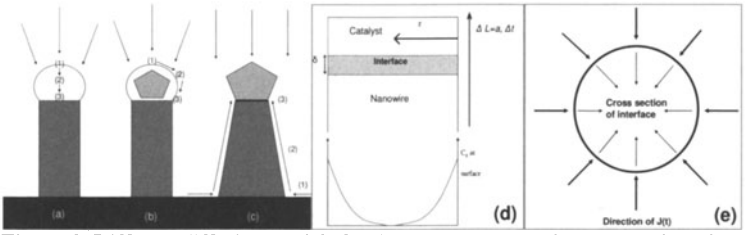

Figure 3. Different diffusion models for the source atoms to incorporate into the growth front of the nanowire. **(a).** The classical VLS. **(b).** The metal droplet is in partially molten state. Its surface and interface are liquid, while the core of the droplet may be solid. **(c).** The metal catalyst is solid, but the interface is liquid. **(d)**.The schematic concentration profile of the source atoms at the catalytic interface. **(e).** The flux J(t) of the source atoms flowing into the catalytic interface.

In this paper, we propose a model to interpret the growth behaviors of thin nanowires by solid catalysts. This model is based on (i) the catalyst is solid, (ii) the source atoms deposited on the substrate surface and the nanowire surface diffuse along the nanowire side walls and preferentially flow into the catalyst interface to result in the nanowire growth, and (iii) the nanowire growth rate is mainly due to the atomic diffusion through the interface. Figure 3c shows schematically this surface/interface incorporation process. The interface at the solid catalyst is considered as a grain boundary. Since the grain boundary diffusion is slower than the surface diffusion,[14] the growth of the nanowires

in the present model is limited by the interface diffusion. According to the Fisher model for grain boundary diffusion [15], the atom concentration at a grain boundary is described by:

$$c = c_0 \exp(-\pi^{-1/4} \frac{(4D/t)^{1/4}}{(\delta D_{gb})^{1/2}} r) \quad (2)$$

where, D is the volume diffusion coefficient, D_{gb} is the grain boundary diffusion coefficient, δ is the grain boundary width c_0 is the concentration at the surface, r is the radius of the nanowire (see figure 3d). The flux of the atoms flowing into the grain boundary (figure 3e) at time t is:

$$J(t) = -D_{gb} \partial_r c(r,t) \quad (3)$$

where the concentration is quasi-static. Assuming that Δt is the time needed for growing ΔL (one lattice layer of a), then the total number of atoms in ΔL is:

$$N = \pi r_0^2 a\rho = 2\pi r_0 \int_0^{\Delta t} J(t)dt = 2\pi r_0 c_0 \pi^{-1/4} \sqrt{\frac{D_{gb}}{\delta}} (4D)^{1/4} \int_0^{\Delta t} t^{-1/4} dt \quad (4)$$

Then, $$\Delta t = (r_0 \pi^{1/4} \rho \frac{3}{8} \frac{a}{c_0} \sqrt{\frac{\delta}{D_{gb}}} (4D)^{-1/4})^{4/3} \quad (5)$$

and $$\frac{\Delta L}{\Delta t} = \frac{dL}{dt} = \frac{a}{(r_0 \pi^{1/4} \rho \frac{3}{8} \frac{a}{c_0} \sqrt{\frac{\delta}{D_{gb}}} (4D)^{-1/4})^{4/3}} = A \frac{1}{r_0^{4/3}} \quad (6)$$

To estimate the growth rate of ZnSe nanowires versus diameters, we use the following parameters: $D_{gb} = 10^{-12}$ cm^2/s,[14] D= 10^{-16} cm^2/s,[14] $c_0 = 0.95$ atom/nm^2;[16] the lattice parameter for ZnSe is a= 0.567 nm; $\rho = 21.7$ atom/nm^3. Then, *A* is determined to be 0.5 nm$^{7/3}$/s. Comparing to the experimental data, we obtained:

$$v = A \frac{1}{r_0^{4/3}} + C \quad (7)$$

where, C is about 0.012 nm/s which means the constant deposition of the source atoms. This value is consistent with the deposition rate of ZnSe on a flat substrate at about 390 °C in MBE. The diameter-dependence of the growth rate estimated by equation 7 matches our experimental data fairly well (see figure 2a). We noticed that this interface diffusion mechanism is different from that of the surface diffusion controlled mechanism.[6] This is because the surface diffusivity is generally one order higher than that of the grain boundary diffusivity [14], and for the present model, the deposition of the source atoms is mainly controlled by boundary diffusion. For the nanowires with a diameter d > 60 nm, the growth rate calculated by the present model is very low because of the increase of the diffusion length at the catalyst interface. This dramatically lowers the deposition rate of atoms at the central area of the nanowire-catalyst interface. During the VLS growth, the atoms on the catalyst surface should have a high mobility and are in semi-melting state. Therefore, the surface always can capture the source atoms to cause a constant growth of the nanowire. For ultra thin nanowires, the melting points of the catalysts will decrease quickly by increasing their diameters. For the nanowires with diameters larger than 60 nm, the directly impinging atoms on the liquid catalysts will play a dominant role during the growth, and the nanowire growth will be controlled by the classical VLS mechanism.

CONCLUSIONS

This study shows the structural changes of ultra thin ZnSe nanowires grown at low temperatures, and the interesting diameter-dependent growth behavior of these nanowires. Ultra thin ZnSe nanowires can grow at a temperature below the eutectic point, and their growth rate can be elucidated based on the model involving interface incorporation and diffusion, in which the catalysts are solid. The growth rate of the ultra thin nanowires largely deviates from the classical VLS growth and the simulated relationship between the growth rates and nanowire diameters is $V= 1/d^n+ C_0$.

ACKNOWLEDGMENTS

This work was financially supported by the Research Grants Council of Hong Kong (Project Nos. N_HKUST615/06, G_HK021/07,AOE-MG/P-06/06-A) and partially supported by the Nanoscience and Nanotechnology Program at HKUST.

REFERENCES

1. E. I. Givargizov, *J. Cryst. Growth* **31,** 20 (1975).
2. E. I. Givargizov, *Highly Anisotropic Crystal*, (D. Reidel Pub. Co., 1987) pp. 104.
3. T. Y. Tan, N. Li, and U. Gosele, *Applied Physics A-Materials Science & Processing* **78,** 519 (2004).
4. S. Kodambaka, J. Tersoff, M. C. Reuter, and F. M. Ross, *Phys. Rev. Lett.* **96,** 096105 (2006).
5. Y. Cai, S. K. Chan, I. K. Sou, Y. F. Chan, D. S. Su, and N. Wang, *Adv. Mater.* **18,** 109-113 (2006).
6. S. Kodambaka, J. Tersoff, M. C. Reuter, and F. M. Ross, *Science* **316,** 729 (2007).
7. G. Neumann and G. M. Neumann, *Surface Self-Diffusion of Metals, Diffusion Monograph Series*, (Diffusion Information Center, 1972) pp. 105
8. Y. F. Chan, X. F. Duan, S. K. Chan, I. K. Sou, X. X. Zhang, and N. Wang, *Appl. Phys. Lett.* **83,** 2665 (2003).
9. Y. Cai, S. K. Chan, I. K. Sou, Y. T. Chan, D. S. Su, and N. Wang, *Small* **3,** 111 (2007).
10. Z. H. Zhang, F. F. Wang, and X. F. Duan, *J. Cryst. Growth* **303,** 612 (2007).
11. U. Philipose, A. Saxena, H. E. Ruda, P. J. Simpson, Y. Q. Wang, and K. L. Kavanagh, *Nanotechnology* **19,** 215715 (2008).
12. L. E. Froberg, W. Seifert, and J. Johansson, *Phy. Rev. B* **76**, 15340 (2007).
13. W. Seifert, M. Borgstrom, K. Deppert, K. A. Dick, J. Johansson, M. W. Larsson, T. Martensson, N. Skold, C. P. T. Svensson, B. A. Wacaser, L. R. Wallenberg, and L. Samuelson, *J. Cryst. Growth* **272**, 211 (2004).
14. N. A. Gjostein, *Diffusion,* edited by Aaronson, (American Society for Metals, 1973) pp. 241.
15. I. Kaur, *Fundamentals of grain and interphase boundary diffusion*, (John Wiley, 1995) pp. 11,17
16. M. D. Johnson, K. T. Leung, A. Birch, B. G. Orr, J. Tersoff, *Surface Science* **350**, 254-258 (1996)

Mater. Res. Soc. Symp. Proc. Vol. 1144 © 2009 Materials Research Society 1144-LL02-02

Optical Properties of Single Wurtzite GaAs Nanowires and GaAs Nanowires With GaAsSb Inserts

Thang B. Hoang[1], Hailong Zhou[1], Anthonysamy F. Moses[1], Dasa L. Dheeraj[1], A. T. J. van Helvoort[2], Bjørn-Ove Fimland[1] and Helge Weman[1]

[1]Department of Electronics and Telecommunications, Norwegian University of Science and Technology, NO-7491 Trondheim, Norway
[2]Department. of Physics, Norwegian University of Science and Technology, NO-7491 Trondheim, Norway

ABSTRACT

We report results on a low temperature micro-photoluminescence (μ-PL) study of single GaAs nanowires (NWs) and GaAs NWs with GaAsSb inserts. The Au-assisted molecular beam epitaxy (MBE) grown GaAs NWs exhibit wurtzite (WZ) crystal structure with very low stacking fault density. At low temperature (4.4 K), PL emission from single WZ GaAs NWs shows an excitonic band at 1.544 eV, ~25 meV higher in comparison with known zinc-blende (ZB) GaAs band gap energy. The one dimensional heterostructures, GaAs/GaAsSb/GaAs, contain GaAsSb inserts (~20 nm long) inserted in GaAs NWs (~50 nm diameter) and are capped with a radial AlGaAs shell. Due to the type II band alignment at the pseudomorphically strained GaAs/GaAsSb heterojunction, the PL emission observed at ~1.26 eV is believed to be due to the spatially indirect recombination between confined holes in the GaAsSb insert and Coulomb attracted electrons at the GaAs/GaAsSb interfaces. At high excitation power a strong blue shift of the PL energy is observed, characteristic for type II transitions. The realization of WZ GaAs and type II GaAs/GaAsSb core-shell NW heterostructures promise interesting physics as well as potential for developing NW based photonic devices.

INTRODUCTION

Semiconductor NWs have attracted considerable attention because of their potential applications in electronic and opto-electronic devices as well as holding new interesting physical properties.[1-3] III-V semiconductor NWs, such as InP and GaAs NWs, exhibit WZ crystal structure in despite of that most of III-V semiconductor compounds exhibit ZB crystal structure in bulk or thin film form.[4-7] The new WZ crystal structure raises questions about fundamental physical parameters such as band gap energy, exciton binding energy and carrier effective masses of these materials. They also create new possibilities for band-structure engineering in NW based devices, including NW-quantum dot heterostructures which can potentially be used as single photon sources.[8]

In contrast to the case of GaAs NWs grown by metal-organic chemical vapor deposition (MOVCD) where mostly the ZB crystal structure is observed,[9,10] WZ GaAs NWs are normally observed when grown by MBE. Several works have experimentally attempted to examine the band gap and PL emission from WZ GaAs NWs but the results are still inconsistent.[11,12] It is even more challenging to study the optical properties of single NWs, due to the high sensitivity of photo-excited carriers to surface states in GaAs. Another major issue when studying the optical properties of these NWs is the large density of stacking faults which are formed during

the growth. The NWs can also contain segments of ZB GaAs which act as collectors that collect most of the photo-excited carriers.[5]

In this work, we report the optical properties of single WZ GaAs NWs. The results on single pseudomorphically strained WZ GaAs NWs with ZB GaAsSb inserts overgrown by a radial AlGaAs shell are also presented as a demonstration of a type II NW heterostructure. In comparison with the known ZB GaAs band gap energy, our low temperature (4.4 K) μ-PL measurements from single WZ GaAs NWs show a PL emission band at an approximately 25 meV higher energy. This result is consistent with previous theoretical calculations.[13,14] PL measurements on single GaAsSb inserts shows a strong emission band at ~1.26 eV. Power dependence measurements show a strong blue shift (~100 meV) of the PL peak, believed to be caused by the state filling effect that induces a renormalization of the ground state energy due to the increasing Coulomb potential as well as from state filling of higher excited holes in the GaAsSb insert.[15]

EXPERIMENTS

The GaAs NWs were grown in a Varian Gen II Modular MBE system equipped with a regular Al cell, a Ga dual filament cell, and Sb and As valved cracker cells. The GaAs(111)B substrate surface was first deoxidized at 620°C, and then a ~ 200 nm thick GaAs buffer layer was grown. This buffer layer was capped with an amorphous As layer to avoid oxidation during its transfer in ambient air to an electron-beam evaporation system for gold depositions. After de-capping, a ~ 1 nm thick Au film was deposited on the sample surface before the sample was loaded into the MBE system again. Under an As_4 flux of 6×10^{-6} Torr, the substrate temperature was increased to a temperature suitable for GaAs NW growth. At this stage, nano-particles containing Au alloyed with the substrate constituents were formed. GaAs NW growth was initiated by opening the shutter of the Ga effusion cell. The temperature of the Ga effusion cell was preset to yield the required Ga flux.

For GaAs/GaAsSb NW heterostructures, GaAs NWs were grown for 25 minutes and then the Sb shutter was opened to supply an additional Sb_2 flux of 6×10^{-7} Torr. A GaAsSb insert was grown for either 30 s, 10 s or 5 s (in different samples), followed by a one minute growth interruption under As_4 flux and then by 10 minutes of GaAs NW growth. The GaAs/GaAsSb NWs were grown under a Ga flux of 4.4×10^{-7} Torr and a substrate temperature of 540°C. In order to suppress non-radiative surface recombination, an AlGaAs shell was grown under As_4 flux with an Al:Ga flux ratio of 3:7. The growth time for the AlGaAs shell was 10 minutes. Finally, a GaAs capping shell was grown (2 minutes) in order to prevent oxidation of the AlGaAs shell.

μ-PL measurements were carried out using an Attocube CFMI optical cryostat. Samples were placed in a He exchange gas with a temperature kept at 4.4 K. Single NWs were excited by a 633 nm HeNe laser line. The laser was defocused onto the samples with an excitation density varied between 0.1-10 $kWcm^{-2}$ using a 0.65 numerical aperture objective lens. The μ-PL from single NWs was collected by the same lens and dispersed by a 0.55 m focal length Jobin-Yvon spectrograph and detected by an Andor-Newton thermo-electric cooled Si CCD camera. The spectral resolution of the system is ~200 μeV. For single NW measurements, NWs were removed from their grown substrate and dispersed on a Si substrate with an average density of ~0.1 NW per μm^2.

DISCUSSION

GaAs nanowires

Figure 1a) shows a transmission electron microscopy (TEM) image of a representative GaAs NW with a low density of stacking faults. In Figure 1b), a high resolution TEM (HRTEM) image of the same NW shows a high quality crystal structure. The diffraction image pattern in the inset of Figure 1b), indicates a pure WZ crystal structure for this NW. μ-PL were measured on single NWs from the same sample from which the TEM images in Figures 1 were taken. Figure 2 shows PL spectra of several single WZ GaAs NWs at 4.4 K. The excitation power was 1 kW/cm^2 and defocused to a spot size of around 5 μm so that individual NWs are entirely excited.

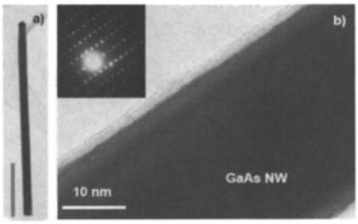

Figure 1. a) TEM image of a stacking fault free GaAs NW. b) HRTEM image and diffraction pattern (inset) shows WZ crystal structure. The scale bar in a) is 500 nm.

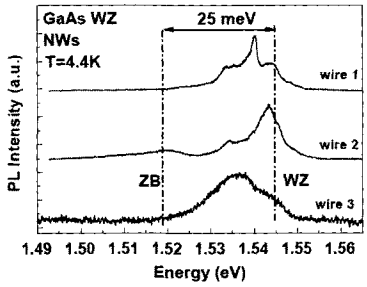

Figure 2. PL spectra from three single NWs. Note that wire 2 shows emissions from both ZB and WZ energies while wires 1 and 3 show only WZ.

The PL emissions from all these NWs exhibit a broad emission band centered at ~1.539eV. The PL spectra display a full width at half maximum (FWHM) of ~11 meV with several features as will be discussed in detail below. All three NWs (wires 1 through 3) show an emission peak near1.545 eV. We suggest this is the free exciton emission of WZ GaAs NWs. This is in consistence with earlier theoretical works[13,14] but in conflict with some recent works (for example, see refs. 11,12,16).

Wire 1 exhibits a narrow emission line at 1.539 eV which might result from excitons bound to defects. The lower energy peaks (between 1.535 and 1.538 eV) which appear in all NWs are probably impurity related recombination peaks. We note that in the PL spectrum of wire 2 there is an emission peak at ~1.518 eV. This emission energy is close to the free exciton emission in ZB GaAs NWs. However, in wires 1 and 3, there are no indications of emission in this energy range. We suggest that this weak emission is associated with ZB GaAs segments in NWs which have a low density of stacking faults. This result is consistent with HRTEM images which show that some NWs exhibit pure WZ free of stacking faults, while other NWs exhibit low density of stacking faults that contain a few ZB GaAs segments.

GaAs nanowires with GaAsSb inserts

As we have reported earlier, WZ GaAs NWs with defect free ZB GaAsSb inserts can be grown expitaxially.[17] Figure 3 shows a scanning electron microscopy (SEM) image of a GaAs/GaAsSb/GaAs NW sample which has been coated with an AlGaAs shell so that the NW heterostructure is pseudomorphically strained. As can be seen in the SEM image, the NWs are straight with a uniform diameter (~ 90 nm including the AlGaAs shell). In addition, the NW density is rather dense and the NW length exhibits a large variation.

In Figure 4a) we plot PL spectra of three GaAs NWs with GaAsSb inserts (labeled A, B and C). As mentioned above, these NWs are coated with an AlGaAs shell therefore their PL intensities are typically two orders of magnitude higher in comparison with the same structure without a shell (not shown here). We note that the PL emission from the GaAs parts of the NWs (Figure 4a) exhibit emission energies close to the ZB band gap energy of GaAs rather than WZ energy as presented in previous section. This is probably due to the presence of stacking faults and ZB GaAs segments contained in this sample. Such ZB GaAs segments are likely to trap most of the photo-excited carriers and therefore emission near the ZB GaAs band gap energy is mostly observed.

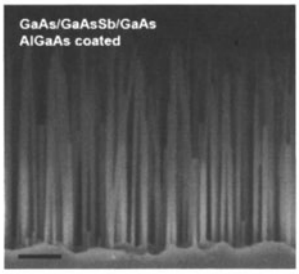

Figure 3. SEM image of a GaAs/GaAsSb/GaAs NW sample (coated with AlGaAs shell). The scale bar is 500 nm.

The emissions from the GaAsSb inserts exhibit a relatively broad band at lower energy (~1.26 eV) and appear to have some variation in energy from wire to wire. This emission is believed to be due to the spatially indirect recombination (type II band alignment) between holes in the GaAsSb insert and Coulomb attracted electrons at the interfaces (see inset in Figure 4b).